Analysis of local shear effects in brick masonry infilled RC frames

COMPDYN 2013
4th ECCOMAS Thematic Conference on
Computational Methods in Structural Dynamics and Earthquake Engineering
M. Papadrakakis, V. Papadopoulos, V. Plevris (eds.)
Kos Island, Greece, 12–14 June 2013

ANALYSIS OF LOCAL SHEAR EFFECTS IN BRICK MASONRY INFILLED RC FRAMES

L. Cavaleri, F. Di Trapani, M. Papia
Dipartimento di Ingegneria Civile, Ambientale, Aerospaziale e dei Materiali (DICAM).
University of Palermo, Viale delle Scienze – 90128 Palermo, ITALY
liborio.cavaleri@unipa.it

Keywords: infilled RC frames, equivalent strut, micromodel, brick masonry, local shear effects.

Abstract. *Masonry infills panels placed among framed structures meshes have a relevant influence in presence seismic actions in terms of strength stiffness and global displacement capacity. In the case of RC structures, the modifications of internal forces due to infill-frame interaction may be not compatible with surrounding frame members strength especially considering additional shear forces arising at the ends of beams and columns in contact with the panel under lateral actions. Such effects may be in many cases the cause of unexpected brittle collapse mechanisms which compromise the safety of the entire structure. In this paper by means of a double (micromodeling and macromodeling) procedure regarding RC meshes infilled with hollow brick masonry, a parametric study is provided defining a connection between local shear forces in critical frame regions and axial force on diagonal pin jointed strut. Proposed strategy allows to predict effective local shear forces using the simple macromodeling approach to reproduce the effect of masonry infills in models.*

1 INTRODUCTION

Masonry infill panels are largely diffused in the common building practice of framed structures even if they are usually considered as non-structural elements. By the observation of seismic damage on infilled frames structures and as largely documented by several analytical and experimental studies in the last decades, it is clear that frames and infills have a strong interaction under seismic load that is not always possible to consider as beneficial for structural safety.

The infilled meshes show, respect to bare ones, a significant increasing of lateral strength and stiffness. However global predictions extended to a whole structural complex are not easy to perform without specific analyses because these depend on the effective distribution of infills among structural meshes.

If planar distribution is regular and approximately symmetric, the contribution given by infill panels is generally beneficial especially in the case of buildings designed to resist to gravity loads only. Conversely irregular planar or elevation distributions are potentially dangerous being often the cause of additional torsional effects and soft story mechanisms activation respectively.

Another relevant aspect to consider in frame-infill interaction regards the modification of internal forces caused by the infills on the adjacent RC members and constitutes the central topic of this paper. As well known, in presence of lateral actions, the panel has a detachment from the infill, remaining in contact with this only in correspondence of the two opposite corners (Fig. 1).

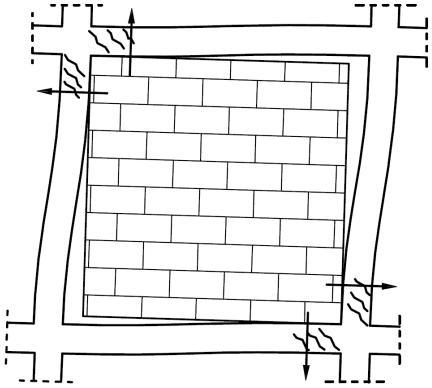

Figure 1. Transmission of local shear forces in infilled frames nodal regions in presence of seismic actions.

Lateral force increasing that occurs on infilled frames because of their higher stiffness is however allowable if RC members adjacent to panels (beams, columns and joints) have sufficient shear strength to avoid local failures.

Especially in the cases of strong infills combined with low shear reinforced frames, local collapse mechanisms are possible to activate compromising global capacity and safety of the entire structure. In Fig. 2 some examples of local shear failure mechanisms due to interaction with infills are reported.

Several authors proposed strategies to reproduce infills effects in structural models. Among these the most employed refer to the macromodel approach which is based on the substitution of the infill by means of an equivalent diagonal concentric pin jointed strut. Such approach, introduced for the first time by Holmes (1961) [1] and suddenly developed by other researchers Stafford Smith (1966) [2], Stafford Smith and Carter (1969) [3], Mainstone (1974) [4], Angel et al. (1994) [5], Papia et al. (2003) [6], has a good reliability in modelling of stiffening

effects produced by panels but is unable to provide any prediction about infill – frame interaction effects in nodal regions.

More complex macromodels, able to reproduce these aspects by means of two or three diagonal struts were also developed by Crisafulli et al. (2000) [7], Crisafulli and Carr (2007) [8], Fiore et al. (2012) [9]. Anyway the identification of mechanical properties to attribute to single struts is quite difficult to accomplish since this depends not only on mechanical features of masonry but also on infill – frame stiffness and geometrical ratios. Such difficulties in identification are more relevant when nonlinear analyses should be performed and the attribution of monotonical or cyclic nonlinear laws for multiple struts is required.

Figure 2. Local shear failures of frames due to interaction with infills under seismic loads.

Conversely to above mentioned methods, others authors Mallik and Severn (1969) [10], Mehrabi and Benson Shing (1997) [11], Benson Shing et al. (2002) [12], Gosh et al. (2002) [13], Asteris (2008) [14], Koutromanos et al. (2011) [15] adopted micromodeling approach to reproduce infill – frame interaction. In these cases panel and frames are modelled using planar shell finite elements while infill – frame contact regions are governed by means of interface elements able to reproduce frictional effects and infill – frame detachment. This kind of approach, that is surely more accurate, gives the best results in terms of local effects and global internal force distribution but, also in this case, the calibration of models and the attribution of interface laws is not easy to accomplish being often not well known all mechanical properties of infill masonries that depend moreover on manufacturing and constructive modalities. Besides the analyses of framed structures which involve micromodels require a so high computational effort to be unacceptable for practical engineering uses.

Interaction between infills and RC frames is also treated by technical codes. Eurocode 8 [16] in the section devoted to modelling in structural analysis prescribes that infill walls which contribute significantly to the lateral stiffness and resistance of building should be taken into account. Then, in the section regarding irregularities in plan, it is stated that infills should be included in the model and a sensitivity analysis regarding the position and the properties of the infills should be performed. Then, with reference to non-uniform distribution of infills in elevation, if a more accurate model is not used, one can calculate the seismic action effects on columns by amplifying them by the magnification factor η calculated as:

$$\eta = 1 + \frac{\Delta W_{Rw}}{\Delta W_{Sd}} \tag{1}$$

where ΔW_{Rw} is the strength reduction of considered storey respect to the upper infilled one and ΔW_{Sd} is the sum of the seismic shear forces acting at the top of considered storey.
Although many times the use of a reliable model is recommended, no models for the infill are included in Eurocode 8 as a support for practical applications, leaving designers free in choosing a criterion for modelling infills and identifying the complex frame-infill interactions.

In a similar way Italian technical code, D.M. 14/01/2008 [17], suggest to amplify forces in potentially soft storeys multiplying by a magnification factor which have a fixed value of 1.4 but also in this case no modelling criteria are given.

Unlike Eurocode 8 and Italian codes, the Federal Emergency Management Agency (FEMA) code 356 [18] explains clearly enough how to take infills into account: the effect of infills has to be considered by a FEM analysis or, alternatively, by introducing a diagonal pin-jointed strut equivalent to the infill. For the first option no more is said, unlike according the second one is specified that the equivalent strut should have the same thickness and modulus of elasticity as the infill panel (but it is not clear along which direction the modulus of elasticity must be calculated) while the width w is given by the following equation:

$$w = 0.175 \left(\lambda_1 h'\right)^{-0.4} d \tag{2}$$

where, with reference to Fig. 3, h' is the height of the frame, measured between the centrelines of the beams, d is the measure of the diagonal dimension of the infill and λ_1 is given by the equation:

$$\lambda_1 = \left[\frac{E_d t \sin 2\theta}{4 E_f I_c h} \right]^{\frac{1}{4}} \tag{3}$$

in which t is the thickness of the infill, h and ℓ are its height and length, respectively, $\theta = atan(h/\ell)$, I_c is the moment of inertia of the columns, E_d and E_f are Young's modulus of the infill and of the material constituting the frame, respectively.

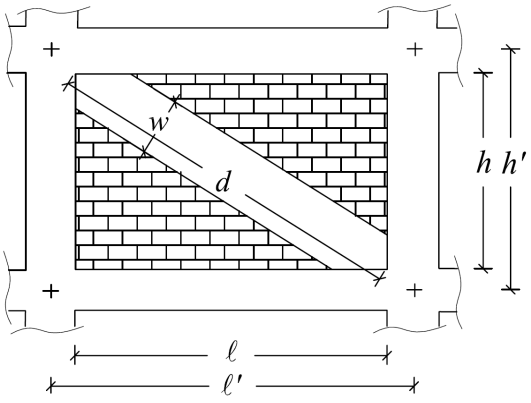

Figure 3. Geometrical features of infill-frame system for the identification of equivalent diagonal strut.

The FEMA code also specifies that beams and columns adjacent to infills should have sufficient strength to support local shear effects arising from the infill – frame interaction in presence of lateral actions. When more accurate analyses are not performed FEMA code states that flexural and shear strength of beams and columns in nodal regions should exceed

the internal forces evaluated by the application, at a specified length (Eqs. 3-4), of the horizontal and vertical components of the axial force in equivalent struts (Fig.4).

$$l_{ceff} = \frac{w}{\cos\theta_c}; \quad \tan\theta_c = \frac{h - l_{ceff}}{\ell} \tag{4}$$

$$l_{beff} = \frac{w}{\sin\theta_b}; \quad \tan\theta_b = \frac{h}{\ell - l_{beff}} \tag{5}$$

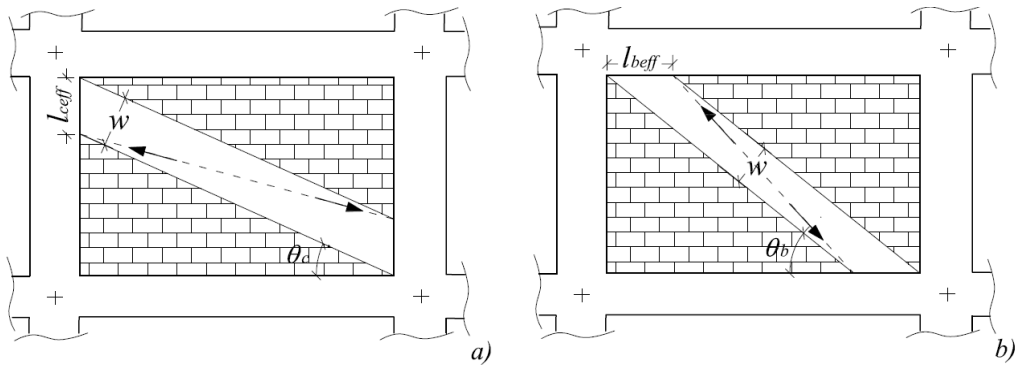

Figure 4. Schemes for evaluation of local effect according to FEMA 356: a) on columns; b) on beams.

A second condition should be verified calculating shear request in the case of formation of a possible ductile mechanism which originates by the activation of plastic hinges at the ends of the reduced lengths l_{ceff} and l_{beff}.

Despite the question of local failure of RC members adjacent to infills is treated in FEMA 356 more the other codes do, the modalities suggested for the evaluation of local effects do not derive form an effective evaluation on the model and may lead to possible overestimations of additional local effects to consider.

Taking into account what above mentioned, a strategy for the evaluation of effective local shear effects when single equivalent strut macromodels are used is developed in this paper.

Masonry typology constituting infill panels which is object of the actual study is hollow brick masonry as defined in ASTM C652 REV A [19].

Infilled meshes which are object of investigation are reproduced by means of two equivalent models in order to compare results: the first one (M1) which provides the use an equivalent concentric braced strut, the second (M2), which makes use of plane shell elements to model infills, nonlinear beam elements to model beams and columns and multilinear elastic links (*MElink*) resisting to compression only to model infill – frame interfaces. Comparisons are carried out varying mechanical features, geometry and stiffening ratios between frame and infill, evaluating for fixed interstorey drifts, the relationship between the axial force evaluated on equivalent strut in M1 model and shear forces evaluated in critical sections of beams and columns in M2 model. The final scope is the definition of a tool which permits to use the simple equivalent concentric strut approach as reference model for the analysis, being able to provide adequate correction coefficients for local shear forces arising in nodal regions.

2 FEM MODELLING

2.1 Models definition

As above mentioned the results of this work are based on the comparison between two different approaches to model same structural system. Referring to a generic infilled mesh, hav-

ing geometrical features indicated in Fig. 5, the responses for a fixed interstorey drift are compared for both M1 and M2 modelling approaches. The M1 model (Fig. 6a), based on the identification of an equivalent diagonal concentric strut replacing panel has a better performance in term of required computational effort. Nevertheless local shear effects on the RC members adjacent to the panel are not evaluable by means of this model. The M2 model (Fig. 6b) requires conversely a higher computational effort but it allows to determine the effective internal forces distribution on RC members trough micromodeling of panels, which are connected to beams and columns trough interfaces elements.

The two models are considered equivalent and comparable when they exhibit the same stiffness both in linear and nonlinear field. More generally stiffness equivalence is defined as function of interstorey drift (d_r) and expressed by the equation:

$$K_{M1}(d_r) = K_{M2}(d_r) \tag{6}$$

$K_{M1}(d_r)$ and $K_{M2}(d_r)$ being the lateral stiffness of M1 and M2 model for assigned d_r.

The identification of M1 and M2 models is afterward exposed while comparing procedures and results are discussed in the subsequent sections.

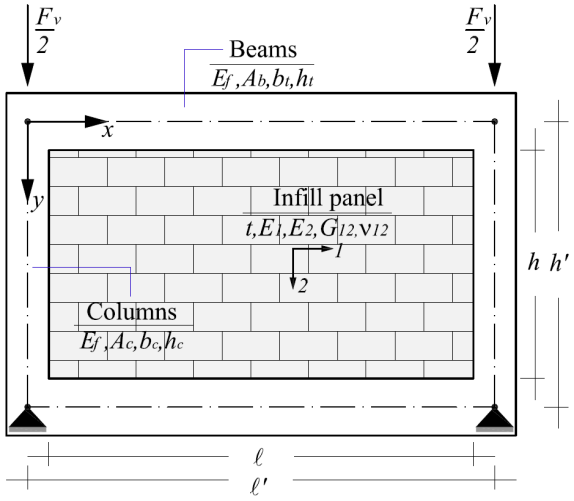

Figure 5. Generic features for an infilled mesh.

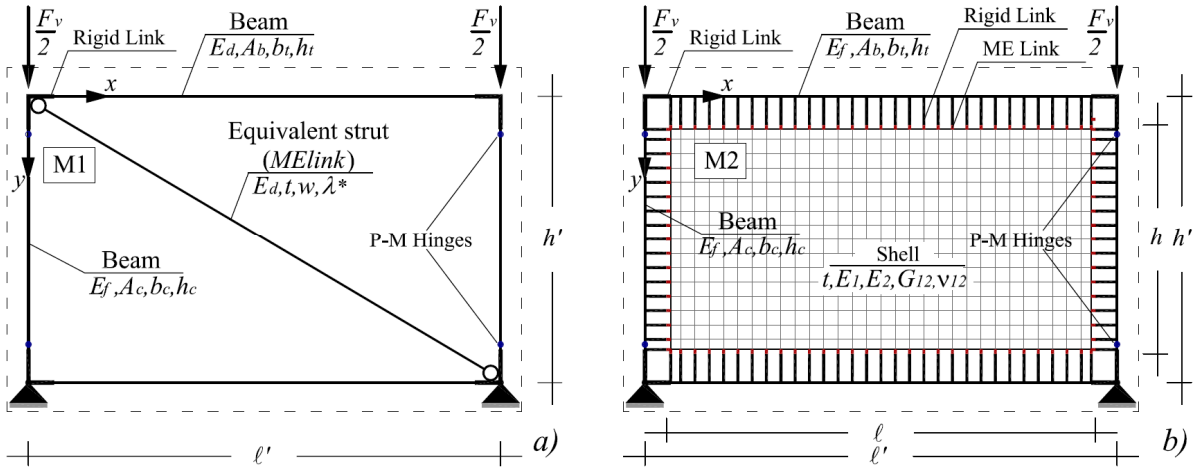

Figure 6. Modelling of infilled mesh: a) M1 model; b) M2 model.

2.2 M1 Model

The M1 model, represented in Fig. 6a, simulates RC infilled mesh having geometrical and mechanical characteristics reported in Fig. 5, in which b_t and h_t are width and depth of beams cross sections respectively and A_b the resultant area while b_c and h_c are width and depth of columns cross sections respectively and A_c the resultant area. The elastic Young modulus of concrete is indicated as E_f. Masonry infills are mechanically characterized by the parameters E_1, E_2, G_{12}, ν_{12} which are respectively the elastic Young modulus, shear modulus and Poisson ratio referred to directions 1 and 2. Equivalent diagonal strut cross section height w is identified through the below reported expression [6]:

$$w = d\,\kappa\frac{c}{z}\,\frac{1}{(\lambda^*)^{\beta}} \tag{7}$$

in which coefficients c and β depends on Poisson ratio ν_d along the diagonal direction and are defined by the below reported equations.

$$c = 0.249 - 0.0116\,\nu_d + 0.567\,\nu_d^{\,2} \tag{8}$$

$$\beta = 0.146 + 0.0073\,\nu_d + 0.126\,\nu_d^{\,2} \tag{9}$$

while the coefficient z depends on panels shape and is evaluable as:

$$z = 1 + 0.25(\ell / h - 1) \tag{10}$$

In Eq.(7) the coefficient k takes into account the effect of the vertical loads involving infill panels. This can be obtained as function of the vertical deformation on columns ε_v due to compressive load F_v (Amato et al. (2008) [20]) through the equation

$$\kappa = 1 + (18\lambda^* + 200)\varepsilon_v : \tag{11}$$

ε_v being evaluated as:

$$\varepsilon_v = \frac{F_v}{2A_cE_f} \tag{12}$$

The parameter λ^* (Eqs. (7) and (11)), which characterize stiffness ratios between infill and frame is finally defined as:

$$\lambda^* = \frac{E_d}{E_f}\frac{t\,h'}{A_c}\left(\frac{h'^2}{\ell'^2} + \frac{1}{4}\frac{A_c}{A_b}\frac{\ell'}{h'}\right) \tag{13}$$

Masonry elastic Young modulus E_d and Poisson ratio ν_d along diagonal direction can be expressed as function of the above defined mechanical parameter (E_1, E_2, G_{12}, ν_{12}) as suggested in Cavaleri et a. (2013) [21].

The equivalent strut constitutive law is defined by a trilinear force-displacement compressive diagram with no tensile strength (Fig. 6). The initial elastic stiffness K_1 evaluated as:

$$K_1 = \frac{E_d t w}{d} \tag{14}$$

while strength at elastic limit F_1 is defined as function of α parameter as follow:

$$F_1 = \alpha F_2 \tag{15}$$

Stiffness in post elastic branch K_2 is instead related to the parameter β as:

$$K_2 = \beta K_1 \tag{16}$$

Elastic limit and peak strength displacements are therefore directly identified:

$$\delta_1 = F_1 / K_1; \qquad \delta_2 = \delta_1 + (F_2 - F_1) / K_2 \tag{17}$$

The softening branch is linearized by connecting points F_2-δ_2 and F_3-δ_3, since F_3=0.7S_2 and δ_3 is obtained by the following expression (Cavaleri *et al*. (2005) [22]):

$$\delta_3 = \frac{1}{\zeta} ln\left[\frac{S_2}{S_3} exp(\zeta\delta_2)\right] \tag{18}$$

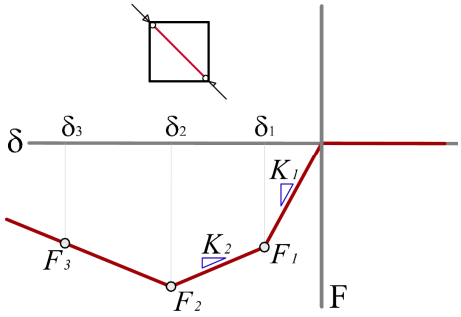

Figure 6. Force – displacement law for equivalent diagonal strut.

Peak strength F_2 of equivalent strut is determined as function of mean shear strength of the panel f_{v0m} as follow:

$$F_2 = f_{v0m} t \tilde{d} \tag{19}$$

in which $\tilde{d}$ represent the ideal diagonal dimension of the panel and is introduced in order to take into account a shear strength reduction due to its aspect ratio. The ideal dimension $\tilde{d}$ is calculated as a fraction of the effective diagonal length d of the panel as shown by means of the reduction factor ψ (Eq. (20)).

$$\tilde{d} = \psi d \tag{20}$$

ψ being obtained as:

$$\psi = \frac{h\sqrt{2}}{\sqrt{(h^2 + \ell^2)}} \tag{21}$$

Table 1 shows $\tilde{d}$ values calculated by substituting Eq. (21) in Eq. (20) for ℓ/h ratios *1, 1.5* and *2*.

ℓ/h	$\tilde{d}$
1.0	d
1.5	0.78 d
2.0	0.63 d

Table 1. Equivalent diagonal length dimensions for different ℓ/h ratios.

The case of collapse for crushing of the corners units in contact with the frame is conservatively here not considered.

The frame mechanical nonlinearities are introduced by means of 4 interacting axial force – bending moment plastic hinges (P-M) defined considering the effective cross section rein-

forcement and geometrical dimensions. Nodal regions at the intersections between beams and columns are modelled as rigid links.

Values adopted for parameters α, β and ζ, defining constitutive law shape for the equivalent diagonal strut, are the same of those proposed in Cavaleri et al. (2012) [23] for hollow brick masonry infills. Besides, basing on results reported in [22], is assumed that the elastic Young modulus ratio $\gamma=E_1/E_2$ is equal to *0.75*, shear modulus $G_{12}=0.4E_2$, Poisson's ratio $\nu_d \cong \nu_{12}=0.1$ while shear strength f_{v0m} of panels is *1.07 MPa* as noticeable by the experimental tests. The above mentioned parameters governing equivalent strut compressive law are summarized in Table 2.

α	β	ζ	f_{v0m} [Mpa]
0.4	0.15	0.02	1.07

Table 2. Parameters defining equivalent diagonal strut constitutive law.

2.3 M2 Model

Referring to the generic infilled mesh (Fig. 5a), the M2 model was also defined (Fig. 5c) providing micromodeling of infill panel by means of orthotropic elastic shell elements identified by the elastic Young moduli E_1 and E_2 along the two orthogonal directions, shear modulus G_{12} and Poisson ration ν_{12}. Modelling of RC beams and columns and plastic hinges is the same of M1 model. The distance between infill panel and surrounding frame beam elements is covered by means of null weight rigid links while mortar joint are modelled as interface elements. Rigid links have the unique function to transmit at each joint the mutual interface infill – frame forces. A similar approach is also proposed in Doudomins (2007) [24]. Interface elements are modelled using *multilinear elastic link* elements having only axial stiffness, no tensile strength and a constitutive law that is assumed elastic in compression. As above mentioned the interface elements are used to simulate mortar joints between masonry infills and RC frames. Taking into account the high manufacturing variability affecting the realization of these interface joints, a conventional elastic Young modulus $E_m=3000$ *MPa* and a conventional joint thickness $h_m=20$ *mm* is fixed. Considering that under lateral loads the infill – frame contact lengths are strongly reduced and mortar interface joints undergo a significant damaging, frictional effects are not included in the model. Moreover other studies (e.g. [9]) demonstrate that friction arising in interfaces is not decisive on the overall response.

Nonlinearity of shell elements, used to model infill panels, is introduced by iteratively modulating an equivalent thickness of masonry. The latter corresponds to the ideal thickness which allows to gain for M2 model, the same lateral stiffness exhibited by M1 model for a fixed interstorey drift.

The M2 model furnishes more detailed results being able to simulate both interface detachment and local shear effects on RC members ends.

3 PARAMETRIC ANALISYS

3.1 Models comparison procedure

As defined in section 2.1, the comparability of the models is possible when they exhibit the same stiffness at a generically assigned interstorey drift. The steps that make up the procedure used to evaluate local shear effects produced by infill panels on RC surrounding frames are below exposed: *a)* assignment of the mechanical properties and geometry of infilled mesh; *b)* choice of a reference interstorey drift (d_r); *c)* definition of M1 equivalent strut macromodel; d) definition of M2 micromodel in which thickness (t) of infill is initially set equal to the real thickness; *e)* identification of the level of damage in M2 model (iteratively reducing infill

thickness) restituting the same secant stiffness exhibited by M1 model (the damage of the frame is uniquely defined by assigning the drift ratio)*; f)* evaluation of effective RC frame internal forces on M2 model.

3.2 Experimental validation of models

In order to verify reliability of the models used to accomplish analyses, an experimental/analytical validation is preliminary performed on the basis of experimental results proposed by Cavaleri et. al (2012) [23], who investigated on the cyclic behaviour of hollow brick masonry infilled frames (Fig. 7). Experimental secant stiffness shown by specimens in cyclic tests are compared, for different drift levels, with those exhibited models M1 and M2 at the same drifts. Geometrical and mechanical characteristics of specimens are reported in Table 3.

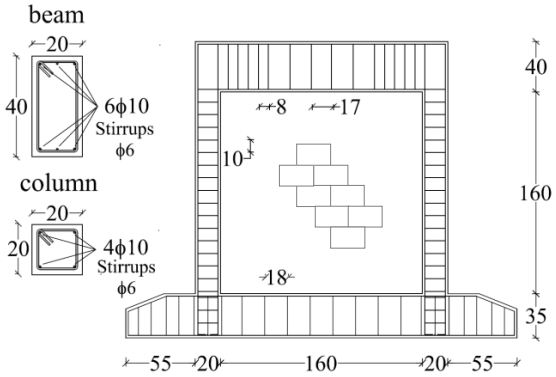

Figure 7. Hollow brick masonry infilled frame specimens details (Cavaleri et. al., 2012 [23]).

h_c [mm]	b_c [mm]	h_t [mm]	b_t [mm]	h [mm]	h' [mm]	ℓ [mm]	ℓ' [mm]
200	200	200	200	1600	1800	1600	1800
t [mm]	f_{v0m} [Mpa]	E_1 [Mpa]	E_2 [Mpa]	G_{12} [Mpa]	ν_{12}	E_f [Mpa]	F_v [kN]
150	1.07	6401	5038	2550	0.07	25000	400

Table 3. Geometrical and mechanical features of hollow brick masonry infilled frames specimens (Cavaleri et al., 2012 [23]).

Interstorey drifts selected for validation of M1 and M2 models are representative of three fundamental conditions of the overall response of the system: elastic phase (d_r*=0.03%*), post-elastic phase (d_r*=0.1%*) and peak strength (d_r*=0.6%*). The comparison between the experimental medium K_{SPM} secant stiffness of tested specimens and numerical secant stiffness K_{M1} and K_{M2} exhibited by models, provided the results reported in Table 4 for the previously defined interstorey drifts.

d_r [%]	K_{spm} [kN/mm]	K_{M1} [kN/mm]	K_{M2} [kN/mm]
0.03	125	130	112.6
0.1	62.50	66.1	67.2
0.6	17.6	16.64	16.55

Table 4. Comparison between experimental medium secant stiffness of specimens (Cavaleri et al., 2012 [23]) and M1, M2 models stiffness for different drift levels.

3.3 Parametric analysis

Parametric analyses afterwards discussed are carried out to evaluate the responses, for assigned damage level (identified by interstorey drift ratio), of infilled systems modelled by means of both the above described approaches. Geometrical and mechanical properties of frames and infills are varied in order to evaluate their influence on the distribution of shear forces occurring on beams and columns ends in contact with infills.

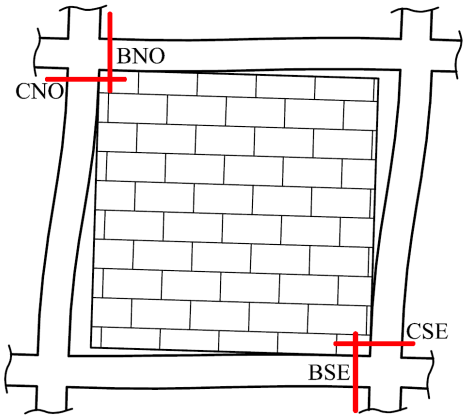

Figure 8. Critical section on RC frame.

With reference to Fig. 8, four critical sections can be identified as the most affected by local shear effects due to infill – frame interaction: BNO (Beam Northwest), BSE (Beam Southeast), CNO (Columns Northwest), CSE (Columns Southeast).

For each considered infilled mesh M1 and M2 models were generated and compared for a fixed drift by means of the previously described procedure. The below reported dimensionless quantities can be thus evaluated:

$$\alpha_{BNO} = \frac{V_{BNO}^{(M_2)}}{N_p^{(M_1)}}; \alpha_{BSE} = \frac{V_{BSE}^{(M_2)}}{N_p^{(M_1)}} \tag{22}$$

$$\alpha_{CNO} = \frac{V_{CNO}^{(M_2)}}{N_p^{(M_1)}}; \ \alpha_{CSE} = \frac{V_{CSE}^{(M_2)}}{N_p^{(M_1)}} \tag{23}$$

in which $N_P^{(M_1)}$ is the axial force on the equivalent diagonal strut evaluated in M1 model while $V_{BNO}^{(M_2)}$, $V_{BSE}^{(M_2)}$, $V_{CNO}^{(M_2)}$, $V_{CSE}^{(M_2)}$ are shear forces in critical sections evaluated in model M2.

In this way, the coefficients α_{BNO}, α_{BSE}, α_{CNO}, α_{CSE} define the relationship existing between shear forces on frame critical sections and axial force on the equivalent strut. If their prediction is possible a priori, they become a useful tool to evaluate the effective shear forces on frame sections as a quote of equivalent strut axial force for all cases in which modelling is performed by means of concentric equivalent strut models. The analyses are executed for two different fixed drift levels, which are representative (taking also into account the experimental evidence) of medium damage and peak strength damage (respectively d_{r1}= 0.1% and d_{r2} = 0.6%).

For d_{r1} analyses the parameter λ^* (Eq. (13)) was chosen as representative of the infill – frame system since it takes into account geometrical and stiffness ratios, while for d_{r2} analyses the product $\xi\lambda^*$ was adopted, being $\xi = h_f/h_c$. This difference on the choice of parameters identifying the infilled mesh is due to the fact that the term λ^* is determined by means of an elastic

approach not taking into account the strength ratios between beams and columns. The latter significantly affects coefficients α_{BNO}, α_{BSE}, α_{CNO} and α_{CSE} when high drift levels occur, especially with regard to plastic hinges formation. The term ξ does not exactly define the flexural strength ratio between beams and columns, however is closely related to it as it is defined.

Two sets of numerical specimens, having different infill aspect ratios (*ℓ/h=1.0* and *ℓ/h=2.0*) were analyzed. The geometrical dimensions are indicated in Tables 5-6 together with the terms λ^*, $\xi\lambda^*$ and *w*. Elastic properties are the same of those indicated in §2.1 while reinforcement geometrical ratio is 1% for all columns sections. It was furthermore assumed that beams have a higher flexural strength respect to columns as in the case of structures designed to resist to gravity loads only. Finally a dimensionless axial force *n=0.2* is assigned on columns.

Case	b_c [mm]	h_c [mm]	b_t [mm]	h_t [mm]	h [mm]	ℓ [mm]	λ^*	$\xi\lambda^*$	w [mm]
C1A	200	200	200	400	1600	1600	1.70	3.40	623
C2A	200	200	200	400	1600	1600	3.40	6.80	565
C3A	250	400	250	500	2700	2700	0.85	1.06	1190
C4A	250	400	250	500	2700	2700	1.30	1.63	1190
C5A	250	400	250	500	2700	2700	2.60	3.25	1034
C6A	250	400	250	500	2700	2700	3.00	3.75	1012
C7A	250	400	250	500	2700	2700	2.05	2.56	1067
C8A	600	300	300	500	2700	2700	0.82	1.37	1192
C9A	600	300	300	500	2700	2700	3.00	5.00	1054

Table 5. Numerical models features - *ℓ/h=1*.

Case	b_c [mm]	h_c [mm]	b_t [mm]	h_t [mm]	h [mm]	ℓ [mm]	λ^*	$\xi\lambda^*$	w [mm]
C1B	200	200	200	400	1600	3200	1.10	2.20	757
C2B	200	200	200	400	1600	3200	2.82	5.64	707
C3B	200	400	200	500	2700	5400	1.30	1.63	1362
C4B	200	400	200	500	2700	5400	2.00	2.50	1368
C5B	200	400	200	500	2700	5400	2.80	3.50	1121
C6B	200	400	200	500	2700	5400	0.85	1.06	1450
C7B	200	400	200	500	2700	5400	3.25	4.06	1200
C8B	600	300	300	500	2700	5400	0.82	1.37	1453
C9B	600	300	300	500	2700	5400	2.14	3.57	1293

Table 6. Numerical models features - *ℓ/h=2*.

Results of analyses are reported in Figs. 9-12 and show the relationship between the quantities λ^* and $\xi\lambda^*$ and coefficients α_{BNO}, α_{BSE}, α_{CNO}, α_{CSE} for drift levels d_{r1} and d_{r2}. Analytical best fitting functions are also provided.

It can be observed that for both considered drift levels α – coefficients undergo a reduction when increasing values λ^* and $\xi\lambda^*$. This trend expresses the general tendency of RC frames to receive shear forces quotes on critical sections that are much relevant as higher is frame stiffness with respect to the panel one. Results also show that the influence of panels' aspect ratio (ℓ/h) has a relevant role only for significant drift levels (d_{r2}). In these cases, when horizontal dimension ℓ prevails on height h, local shear effects are significantly more relevant on columns respect to beams.

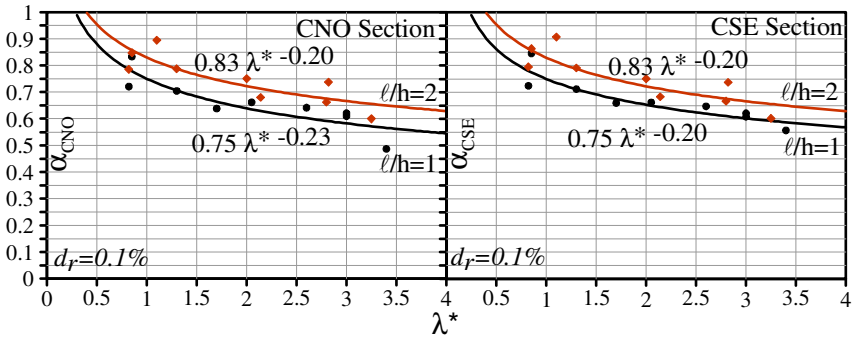

Figure 9. α_{CNO} - α_{CNE} vs. λ^* parametric analysis at d_r=0.1% and best fitting functions.

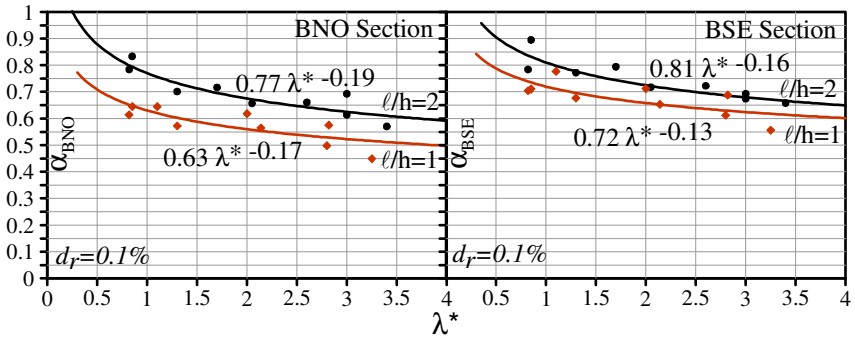

Figure 10. α_{BNO} - α_{BNE} vs. λ^* parametric analysis at d_r=0.1% and best fitting functions.

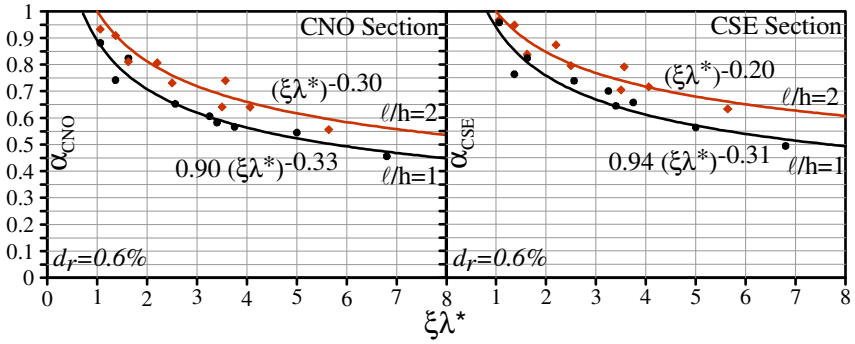

Figure 11. α_{CNO} - α_{CNE} vs. $\xi\lambda^*$ parametric analysis at d_r=0.6% and best fitting functions.

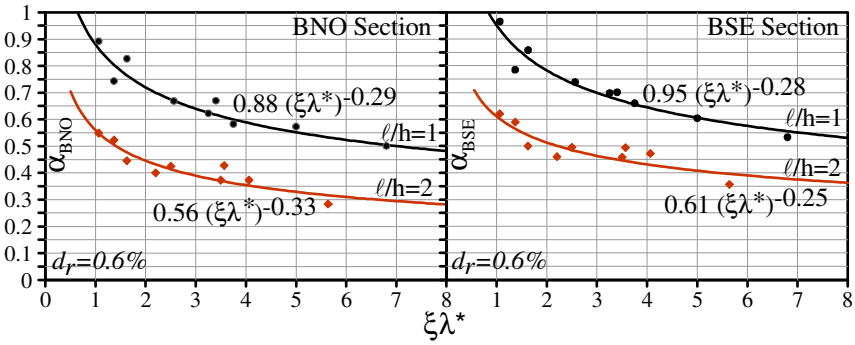

Figure 11. α_{BNO} - α_{BNE} vs. $\xi\lambda^*$ parametric analysis at d_r=0.6% and best fitting functions.

In Fig. 10 a comparison between the response exhibited by models M1 and M2 for a fixed drift is reported in terms of deformed shapes and internal shear forces distribution on RC

frame members evidencing also the strong relevance of local shear effects on critical sections determined by means of M2 model with respect to M1.

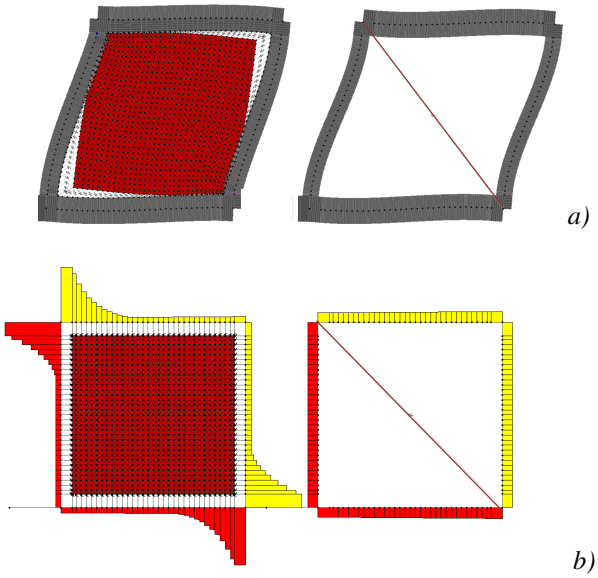

Figure 10. Comparison between M1 and M2 models responses: a) deformed shape; b) shear distribution.

Results of the above reported analyses can be used for verification RC members capacity when linear or nonlinear analyses are performed by means of equivalent concentric strut models. The suggested verification procedure provides first the evaluation of damage level by simply identifying the occurring interstorey drift ratio, the evaluation of the axial force on equivalent strut and subsequently the identification of parameters λ^* and $\xi\lambda^*$ for the reference infilled mesh. Once panel ℓ/h ratio is assigned, coefficients α_{BNO}, α_{BSE}, α_{CNO} and α_{CSE} are univocally identified through the analytical interpolating functions. Shear demand to be considered for verification of critical section V_{BNO}, V_{BSE}, V_{CNO}, V_{CSE} is thus evaluable by means of the following expressions:

$$V_{BNO} = V_0 + \alpha_{BNO} N_P \; ; \; V_{BSE} = V_0 + \alpha_{BSE} N_P \tag{24}$$

$$V_{CNO} = \alpha_{CNO} N_P \; ; \; V_{CSE} = \alpha_{CSE} N_P \tag{25}$$

V_0 being shear force due to the vertical loads on the beams and N_p the axial load on equivalent strut.

4 CONCLUSIONS

The present paper provides a tool for the evaluation local shear forces acting at the ends of beams and columns of hollow brick infilled frames in presence of lateral loads when adopting equivalent concentric strut macromodels.

By means of a parametric analysis, in which the mechanical characteristics of infill – frame systems are varied with the parameter λ^*, α- coefficients are evaluated providing also analytical best fitting functions. The latter permit to express local shear forces on critical sections of beams and columns as a fraction of axial load evaluated on the equivalent strut.

Once verified the substantial dependence of these coefficients on stiffness infill – frame ratio in linear and nonlinear phases, the latter become a predictive tool that is useful to asses

shear demand on RC members critical sections which is otherwise undetectable by means of simple equivalent concentric strut models.

The proposed tool was obtained by considering the mechanical properties of hollow brick masonry infills and primary structure configurations representative of RC frames designed to resist to vertical loads only. The study can be surely improved including the cases of masonry infills having different mechanical properties and seismic designed frames. It is however here possible to point out that a more accurate assessment of local shear effects is achievable even if high detailed and onerous models are not used to perform analyses. Moreover, the procedure here developed, may represent a supplementary instrument to technical codes prescriptions which may be often cause overestimations in evaluation of local infill – frame interaction effects.

AKNOWLEDGEMENTS

This study was sponsored by ReLUIS, Rete di Laboratori Universitari di Ingegneria Sismica, Linea 2, Obiettivo 5: Influenza della Tamponatura sulla Risposta Strutturale.

REFERENCES

[1] M. Holmes, Steel frames with brickwork and concrete infilling, *Proc. of Institution of Civil Engineers*, Paper No.6501:473-478,1961.

[2] B. Stafford Smith, Behaviour of the square infilled frames. *J. Struct. Div. (ASCE)*, **92**(1), 381-403, 1966.

[3] B. Stafford Smith, C. Carter, A method for analysis for infilled frames. *Proc. of Institution of Civil Engineers*, Paper No.7218, 31-48, 1969.

[4] R.J. Mainstone, Supplementary note on the stiffness and strength of infilled frames. *Building Research Station*, UK, Current Paper CP 13/74, 1974.

[5] R. Angel, D. Abrams, D. Shapiro, J. Uzarski, M. Webster, Behavior of Reinforced Concrete Frames with Masonry Infills. *Civil Engrg. Studies, Structural Research Series*. No. 589, UILU-ENG-94-2005, Dept. of Civil Engineering, University of Illinois at Urbana Champaign, 1994.

[6] M. Papia, L. Cavaleri, M. Fossetti, Infilled frames: developments in the evaluation of the stiffening effect of infills. *Struct. Eng. and Mech.*, **16**(6), 675-93, 2003.

[7] F.J. Crisafulli, A.J. Carr, R. Park, Analytical modelling of infilled frames structures –a general review. *Bull. NZ Soc. Earth. Eng.*, **33**(1), 30–47, 2000.

[8] F.J. Crisafulli, A.J. Carr, Proposed macro-model for the analysis of infilled frame structures. *Bull. New Zealand Soc. Earth. Eng.*, **40**(2), 69–77, 2007.

[9] A. Fiore, A. Netti, P. Monaco, The influence of masonry infill on the seismic behavior of RC frame buildings. *Eng. Struct.* , **44,** 133-45, 2012.

[10] D.V. Mallick, R.T. Severn, The behaviour of infilled frames under static loading. *Proc. Inst. Civ. Eng.*, **38**, 639-56, 1967.

[11] A.B. Mehrabi, P.B. Shing, Finite element modelling of masonry-infilled RC frames. *J. Struct. Eng.*, **123**(5), 604-13, 1997.

[12] P.B. Shing, A.B. Mehrabi, Behaviour and analysis of masonry-infilled frames. *Prog. Struct. Eng. Mater.*, **4**(3), 320–31, 2002.

[13] A.K. Ghosh, A.M. Made, Finite element analysis of infilled frames. *J. Struct. Eng.*, **128**(7), 881–89, 2002.

[14] P.G. Asteris, Finite element micro-modeling of infilled frames, *Electronic J. of Struct. Eng.*, **8**, 1-11, 2008.

[15] I. Koutromanos, A. Stavridis, P. Benson Shing, K. Willam, Numerical modeling of masonry-infilled RC frames subjected to seismic loads. *Computers and Structures*, **89**(11-12), 1026-37, 2011.

[16] Eurocode 8, 2004. Design of structures for earthquake resistance - Part 1: General rules, seismic actions and rules for buildings.

[17] D.M. LL. PP. 14 Gennaio 2008, Nuove norme tecniche per le costruzioni.

[18] FEMA 356, 2000. Prestandard and commentary for the seismic rehabilitation of buildings.

[19] ASTM C652 REV A, Standard Specification for Hollow Brick (Hollow Masonry Units Made From Clay or Shale), 2012.

[20] G. Amato, M. Fossetti, L. Cavaleri, M. Papia, An updated model of equivalent diagonal strut for infill panels. *Eurocode 8 perspectives from Italian standpoint, workshop*; Napoli, Italy, 2008.

[21] L. Cavaleri, F. Di Trapani, G. Macaluso, M. Papia, P. Colajanni, Definition of diagonal Poisson's ratio and elastic modulus for infill masonry walls. *Mat. and Struct.* DOI 10.1617/s11527-013-0058-9, 2013.

[22] L. Cavaleri, M. Fossetti, M. Papia, Infilled frames: developments in the evaluation of cyclic behavior under lateral loads. *Struct. Eng. and Mech.*, **21**(4), 469-94, 2005.

[23] L. Cavaleri, F. Di Trapani, M. Papia, Strutture intelaiate e tamponate in c.a.: sperimentazione e sviluppi nella modellazione analitica e numerica. *19° Congresso CTE*, Bologna, Itay, November 8-10, 2012.

[24] I.N. Doudoumis, Finite element modelling and investigation of the behaviour of elastic infilled frames under monotonic loading, *Eng. Struct.*, **29**(6), 1004–24, 2007.